

Structural modifications of the $\text{Gd}_2\text{O}_3(110)$ films on $\text{GaAs}(100)$

C. Steiner, B. Bolliger, and M. Erbudak

Laboratorium für Festkörperphysik, ETH, CH-8093 Zürich, Switzerland

M. Hong, A. R. Kortan, J. Kwo, and J. P. Mannaerts

Bell Laboratories, Lucent Technologies, Murray Hill, New Jersey 07974

(Received 15 May 2000; revised manuscript received 12 July 2000)

We report an fcc structure for the epitaxial Gd_2O_3 films grown on $\text{GaAs}(100)$. This fluorite-derived structure appears to be stabilized by epitaxy with the substrate and has a great similarity to the GaAs structure. A model calculation supports this finding. Our secondary-electron imaging studies of these nanometer-thick films reveal that the films are cubic as deposited, and this structure can be derived from the stable α -phase of the Gd_2O_3 by a mild Ne^+ -ion bombardment and a subsequent anneal. These epitaxial Gd_2O_3 films have great importance because of their excellent surface passivation properties.

Recently, it was discovered that thin films of crystalline gadolinium oxide (Gd_2O_3) grow epitaxially on the $\text{GaAs}(100)$ substrate in a cubic structure that is isomorphic to $\alpha\text{-Mn}_2\text{O}_3$,^{1,2} with its $[110]$ axis oriented along the surface normal. Despite a large mismatch of 3.9% in lattice constants at the interface and grossly different crystal structures, these films were found to be thermodynamically very stable. However, the exact nature of the interface structure and the registry of the film atoms with respect to the GaAs substrate could not be extracted unambiguously from the x-ray diffraction data.

Secondary-electron imaging (SEI) is a powerful real-space probe,³ which is an ideal tool to study this problem. It has a depth resolution of several atomic layers and is particularly sensitive to relative displacements of atoms in crystalline structures. In this work, we have exploited this probe in order to bring a better understanding to the nature of epitaxy at the interface. The Gd_2O_3 layers and their stability are studied by SEI, after exposing the surface to air for prolonged times as well as after heating and bombarding it with noble-gas ions. We found that the crystal structure of the film surface remains stable during heat treatment up to 800 K, but disorders upon sputtering with Ne^+ ions. Subsequent annealing re-establishes the crystallinity in the gadolinium-oxide layer, however, in a fluorite-based cubic structure with the $[100]$ direction parallel to that of the GaAs substrate. SEI reveals that the atomic orientation of the recrystallized film is in registry with the substrate. We have also performed electron-scattering calculations on model structures that simulate experimental results and find good agreement with our measurements.

Crystalline Gd_2O_3 exists in cubic, monoclinic, or hexagonal phases.⁴ The cubic modification has the space group $Ia\bar{3}(T_h^7)$ with a lattice constant of 10.812 Å and 80 atoms per unit cell.⁵ This space group implies the existence of twofold-, threefold-, and fourfold-symmetry axes, while the structure is distantly related to the fluorite type. It can be viewed as an oxygen-vacancy ordered supercell of the fluorite structure. By contrast, GaAs grows in zinc-blende structure with a lattice constant of 5.654 Å.

A 35-Å-thick single-crystal Gd_2O_3 film was grown epitaxially on a $\text{GaAs}(100)$ substrate, using ultrahigh-vacuum (UHV) electron-beam evaporation.¹ It was found that the $[110]$ direction of Gd_2O_3 is aligned parallel to the $[100]$ direction of the underlying GaAs . In addition, the (001) plane of the Gd_2O_3 cell is parallel to the $(0\bar{1}1)$ plane of the GaAs substrate.^{1,2,6} The total area of the sample surface investigated here, exposing the (110) plane of Gd_2O_3 , is approximately $7 \times 7 \text{ mm}^2$. The samples were fabricated and exposed to air for several months before insertion into vacuum.

Structural investigations are performed by SEI in an UHV chamber with a total pressure in the lower 10^{-10} mbar region. In SEI, an electron beam of 2 keV is directed onto the sample surface to excite secondary electrons. Those electrons which are quasielastically backscattered are registered by a display-type collector system, which is concentric with the sample. Since electron-atom scattering at 2 keV concentrates the electron intensity in the forward-scattering direction and the secondary electrons scatter at surface atoms before leaving the sample, the recorded electron intensity shows enhancements corresponding to the atomic rows. Thus, the secondary-electron images carry information on the local atom arrangement in the sample in the form of a central projection of the crystallographic directions. Hence, the relative orientations of the symmetry axes in a given structure can be observed in direct space. In the recorded patterns, bright patches which are closely spaced form a band, signaling the presence of a crystallographic plane. In SEI, three-dimensional views of structures can be acquired by rotating the sample. The patterns originate from a sample depth of about 25 Å under the surface, given by the mean free path of 2-keV electrons.⁷ In the patterns presented here, the central portion of the screen represents the zero polar angle, while its outer edge corresponds to a polar angle of $55 \pm 1^\circ$.

In addition to SEI, low-energy electron-diffraction (LEED) experiments with the same sample were performed by lowering the primary-electron energy while maintaining all other experimental parameters. Auger-electron spectroscopy (AES) was used to determine the chemical composition of the sample.

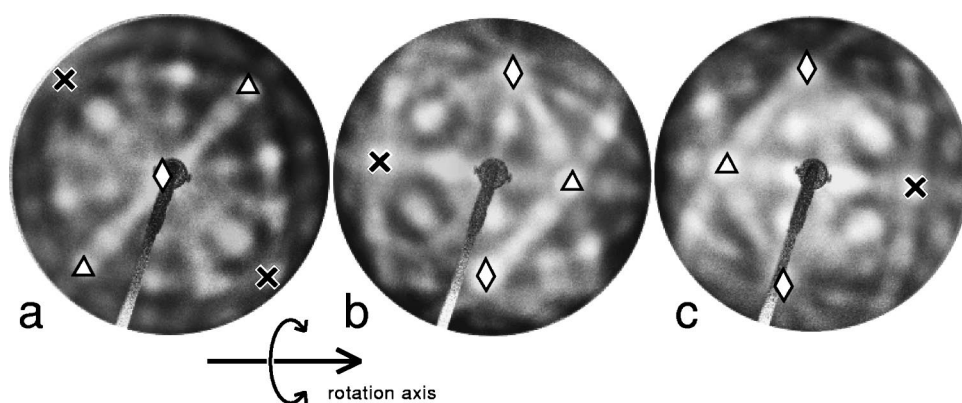


FIG. 1. SEI patterns of the (110) surface of the Gd_2O_3 film. (a) The surface normal coincides with the display axis, (b) and (c) the sample is rotated through 35° around the indicated axis in both directions. The symmetry axes are marked as follow: \diamond = twofold; \triangle = threefold; \times = fourfold.

Figure 1(a) shows the SEI pattern of the untreated, as-received sample oriented such that its surface normal is parallel to the direction of primary-electron incidence. The observed orthogonal symmetry confirms that the twofold-symmetric $[110]$ direction is at the center of the pattern, covered by the shadow of the electron gun. Few low-index directions are indicated. The pattern contains several blurred bands, representing different (hkl) planes. In particular, two mirror planes are found, crossing each other at the center, one going from bottom left to top right, the other one from top left to bottom right. The former, the $(1\bar{1}0)$ plane, contains two patches, each at a polar angle of 35° representing the $[11\bar{1}]$ and $[111]$ directions. The latter represents the (001) plane and contains two fourfold-symmetry axes, each at 45° , the $[100]$ and $[010]$ directions. The symmetry in electron intensity around these patches becomes more apparent if the sample is rotated through a horizontal axis. Thus, a 35° rotation in one direction results in the pattern shown in Fig. 1(b). Here, the horizontal central band is the $(01\bar{1})$ plane and the patch at the top, located on the $(\bar{1}01)$ plane represents the $[101]$ direction. In this view, the fourfold symmetry around the $[100]$ direction and the threefold symmetry around the $[111]$ are clearly detectable. A rotation in the opposite direction produces the pattern in Fig. 1(c) where the $[01\bar{1}]$ direction becomes visible at the bottom of the pattern. The horizontal central band is the (101) plane, containing the fourfold symmetric $[010]$ direction on the right and the threefold symmetric $[11\bar{1}]$ direction on the left.

These patterns are obtained from the sample without any surface treatment. Although the SEI patterns show good definition, no LEED spots can be observed from the sample, implying that one to two top atomic layers are disordered, with prevailing crystalline order in the layers underneath. An attempt to clean the surface by annealing at 800 K neither changed the SEI results nor crystallized the top few disordered layers.

In a previous study,⁸ a metastable fcc phase of Gd_2O_3 was grown on an NaCl substrate. Upon heating to 250°C , it was found that this fcc phase irreversibly transformed to the bcc phase of $\alpha\text{-Gd}_2\text{O}_3$. Our findings extend this thermal stability range up to 800 K. We have next sputtered the surface with Ne^+ ions at an energy of 1 keV for 30 s at an ion-current density of 5×10^{-8} A/mm², while maintaining the sample at 750 K. The diameter of the ion beam at half-maximum intensity was 2 mm with an incidence angle of 60° relative to the sample normal. We estimate that, in these conditions,

atoms corresponding to about 0.3 monolayers (ML) are removed from the surface.⁹ Thus, upon partial removal of the top disordered atom layers, blurred LEED patterns could be observed. Using these patterns, an approximate surface lattice constant of the surface film was derived as 11 Å, which indicates that the structure is indeed cubic $\alpha\text{-Gd}_2\text{O}_3$. Scanning the primary-electron beam over the entire surface both in the SEI and LEED modes did not induce noticeable changes in the quality of the patterns. AES indicated the presence of C and N contamination on the untreated surface, beside Gd and O. No signal of Ga or As could be detected before or after sputtering, because the escape depth of approximately 5 Å for the Auger electrons was considerably less than the thickness of the remaining film. Moreover, the Ne^+ ions were not embedded into the crystal surface at elevated temperatures and the structure remained intact. The SEI patterns were compared with the single-scattering calculations (SSC) applied on the cubic structure of the Gd_2O_3 crystal. This was constructed using the average values of different rare earth oxides.⁵ The computed patterns reproduced all the low-index directions at their expected positions, but not all the bands.

Interestingly, the bands forming the triangles around the threefold-symmetry axes (cf. Fig. 1) did not appear in the calculated results. In the course of searching for a better reproduction of the secondary-electron images, we have found that the simulations did not differ appreciably when certain atomic positions were displaced as much as 0.1 Å around their average value. However, the calculations showed a sensitive dependence on the oxygen content in the structure. Several calculations were performed using model structures with successive oxygen reduction at random sites of the crystal. The best agreement between calculation and experiment was achieved with a Gd-to-O ratio of 1:1. Using this composition, all the bands could be reproduced satisfactorily. Calculated patterns based on this model along the twofold-, threefold-, and fourfold-symmetry axes are shown in Fig. 2. Besides the major symmetry directions, $\langle 100 \rangle$, $\langle 110 \rangle$, and $\langle 111 \rangle$, there can also be found patches that represent directions or planes with higher indices. Some of these and their equivalents are indicated in the figure.

One possible explanation for these observations is that regular oxygen sites in the $\alpha\text{-Gd}_2\text{O}_3$ lattice already exhibit a broad distribution, and small displacements are not expected to change the calculated patterns. By the same token, removing oxygen atoms would only help define the atomic planes better. One can imagine a thin film of $\alpha\text{-Gd}_2\text{O}_3$, where some

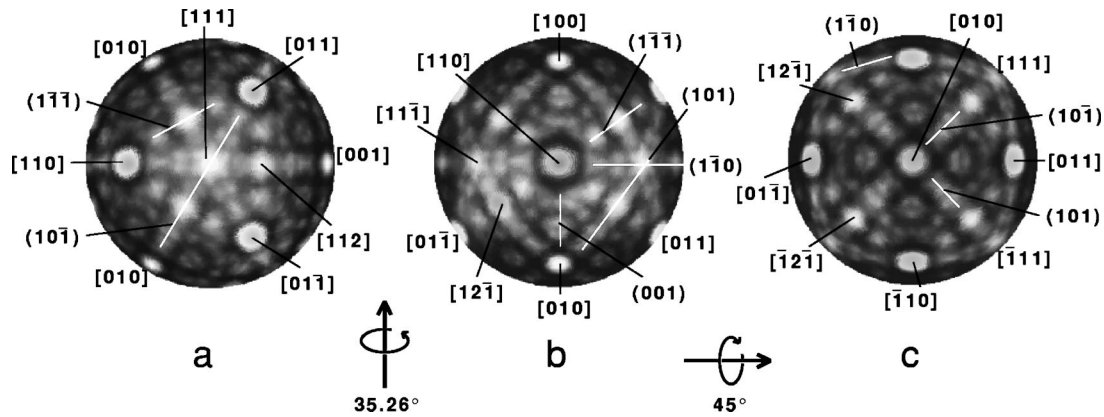


FIG. 2. Results of SSC calculations of the Gd_2O_3 crystal with a reduced amount of oxygen ($\text{Gd}:\text{O} = 1:1$). Different views are shown (a) along the threefold-, (b) the twofold-, (c) and the fourfold-symmetry axes.

of the O atoms are forced to more symmetric sites by the epitaxial conditions. An actual composition change occurring by the loss of oxygen is very unlikely since Gd can only exist in the (+3) valent state. An earlier electron-diffraction experiment has suggested that Gd_2O_3 , when annealed in the presence of metallic Gd, transforms into GdO ,¹⁰ which is now believed to be unlikely.

Significant changes in the SEI pattern were found after the sample was sputtered at room temperature for 15 s at a current density of 5×10^{-7} A/mm², corresponding to removal of 1.5 ML. Neither LEED nor SEI pattern could be observed, signaling the disappearance of the long-range as well as the short-range order in the top few monolayers. The destruction of the crystalline order upon mild sputtering has been encountered in several other ionic crystals and is due to the noble-gas ions implanted into the surface structure. This observation shows that not only shallow surface layers are affected by this treatment, but the disorder prevails at least throughout the escape depth of secondary electrons. Outside the sputtered area the twofold-symmetric pattern could still be observed, because the diameter of the neon-ion beam was smaller than the dimensions of the sample. Hence, the destruction of the surface crystallinity is a local effect and ordered and disordered phases coexist next to each other at the surface.

The crystalline order of the film is partly restored by annealing at 750 K for 10 minutes. An SEI pattern could be observed with reduced contrast, however, LEED patterns remained absent. Figure 3(a) displays a pattern obtained from the film, with the surface normal of the sample aligned along

the display axis. The bands of increased electron intensity and the patches due to interatomic directions are arranged in fourfold-symmetry revealing that the recrystallization of the film produced a cubic structure aligned with its [100] axis parallel to the display axis.

AES performed on the disordered film before annealing as well as on the recrystallized surface after annealing indicated the presence of Gd and O with some C contamination, but not Ga and As. Hence, the observed pattern, shown in Fig. 3(a) cannot originate from the GaAs substrate.

On Fig. 3(b), the secondary-electron pattern obtained from GaAs(100) is displayed. The surface is prepared by extensive sputtering and heating the sample. The overall fourfold symmetry together with the details of the electron-intensity distribution in the pattern are characteristic of a (100) surface of the zinc-blende structure. An SSC calculation for the GaAs structure produces a pattern which closely resembles that shown in Fig. 2(c). There is also perfect alignment between the gadolinium-oxide and GaAs structures indicating that it is the GaAs substrate which dictates the recrystallization mode of the once disordered gadolinium-oxide film.

The cubic Gd_2O_3 structure is closely related to the fluorite structure with two anions per one cation, shown in Fig. 4(a). The cations form an fcc lattice, while the anions fill all the tetrahedral sites. Therefore, each cation has eight anion neighbors and each anion has four cation neighbors. The sesquioxide structure is derived by removing two oxygen anions out of the unit cell, thus reducing the number of anions and doubling the lattice constant.^{2,11} This change in the anion content in the structure leaves the cations in an octa-

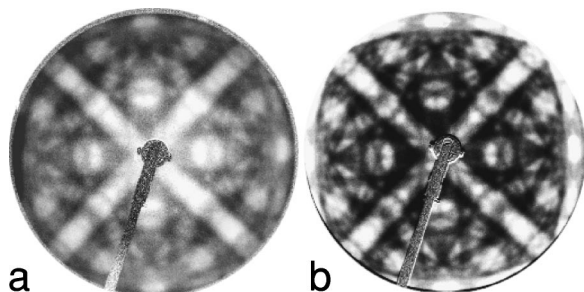


FIG. 3. (a) SEI of fourfold-symmetric surface film, (b) compared with a pattern obtained from the GaAs(100) substrate after removal of the film.

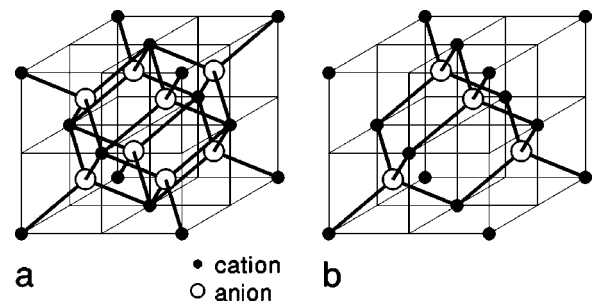


FIG. 4. Comparison of the (a) fluorite and (b) zinc-blende crystal structures.

hedral coordination with some disorder and vacancies in the occupied tetrahedral sites.

Gadolinium oxide in the fluorite structure with the modified oxygen atoms would have a lattice constant comparable with that of GaAs. Therefore, we conjecture that, upon annealing the disordered film, the Gd and O atoms reorganize in the fluorite structure. The formation of this structure is assisted by the GaAs substrate that acts as a structural and chemical template. Consequently, Gd_2O_3 films in this structure are arranged in an epitaxial orientation with the (100) surface of the GaAs substrate.^{2,6} It is essential that the layer be disordered all the way to the interface upon ion bombardment. Only then does the substrate influence the growth of a passivation layer with fourfold-symmetry, as observed. An explanation for the reordering might be that the open and complicated structure of Gd_2O_3 causes the Gd and O atoms to assemble in a simpler and more densely-packed structure. Both unit cells lie congruently on each other, with parallel [100] directions. Probably, the lattice constant of the gadolinium oxide in the fluorite structure has to be modified in order to match the underlying oxygen-terminated GaAs(100).

Figure 4(b) illustrates the zinc-blende structure. Bist *et al.*¹⁰ have suggested the formation of GdO in the zinc-blende structure with a lattice constant of 5.24 Å, upon annealing Gd_2O_3 in the presence of Gd metal. This is the native structure of GaAs, with Ga atoms in the tetrahedral As coordination. Structurally, this phase is the closest one that can account for the fourfold-symmetric films developed upon an-

nealing the disordered film. However, GdO is not an accepted oxide phase of gadolinium.¹² Yet, a comparison between Figs. 4(a) and 4(b) shows the close relation between the fluorite and the zinc-blende structures: the latter is obtained by removing every second oxygen atom in each direction.

The Gd_2O_3 passivation film investigated here is isomorphic with $\alpha\text{-Mn}_2\text{O}_3$ and grows in an epitaxial orientation with the GaAs(100) substrate, aligning its [110] axis with the surface normal. The structure of this film is stable to heat exposures as high as 800 K. In contrast, a mild bombardment with noble-gas neon ions at room temperature completely destroys the crystalline structure. The disordered film recrystallizes in a cubic phase, however, in a structure, unknown to native Gd oxides. We also have found that some of the as-received gadolinium-oxide films displayed fourfold-symmetric structures.¹³ This unexpected phase observed in SEI patterns was not distinguishable from the zinc-blende structure of the GaAs substrate. Apparently, the thin (<25 Å) Gd_2O_3 films have a tendency to grow in a fourfold-symmetric structure on the GaAs (100) surface, both during the initial growth and during the after-growth treatment. We believe that it is the ambient oxygen pressure that keeps $\alpha\text{-Gd}_2\text{O}_3$ stable in the form of atomically thin films.

The authors are thankful to A. Atrei for the phase shifts of Gd, required as input to the SSC, and for his valuable suggestions. This work was supported by the Schweizerischer Nationalfonds.

¹M. Hong, J. Kwo, A. R. Kortan, J. P. Mannaerts, and A. M. Sergent, *Science* **283**, 1897 (1999).

²A. R. Kortan, M. Hong, J. Kwo, J. P. Mannaerts, and N. Kopylov, *Phys. Rev. B* **60**, 10 913 (1999).

³M. Erbudak, M. Hochstrasser, E. Wetli, and M. Zurkirch, *Surf. Rev. Lett.* **4**, 179 (1997).

⁴An account on the different structures of Gd_2O_3 and their transformations is given by C. Boulesteix, in *Handbook Phys. Chem. Rare Earths*, edited by K. A. Gschneidner, Jr. and L. Eyring (North Holland, New York, 1982), Vol. 5, p. 321.

⁵R. W. G. Wyckoff, *Crystal Structures* (Interscience Publishers, New York, 1964), Vol. 2, pp. 2–5.

⁶B. Bolliger *et al.*, *Surf. Interface Anal.* **30**, 514 (2000).

⁷M. P. Seah and W. A. Dench, *Surf. Interface Anal.* **1**, 2 (1979).

⁸A. A. Kashaev, L. Ushchapovskii, and A. G. Il'in, *Sov. Phys. Crystallogr.* **20**, 114 (1975).

⁹*Sputtering by Particle Bombardment I*, edited by R. Behrish, Topics in Applied Physics, Vol. 47 (Springer, New York, 1981).

¹⁰B. M. S. Bist, J. Kumar, and O. N. Srivastava, *Phys. Status Solidi A* **14**, 197 (1972).

¹¹A. R. Kortan, M. Hong, J. Kwo, J. P. Mannaerts, and N. Kopylov, *Mater. Res. Soc. Symp. Proc.* **573**, 21 (1999).

¹²M. Gasgnier and P. Caro, *Cryst. Lattice Defects* **8**, 19 (1978).

¹³B. Bolliger and M. Erbudak (unpublished).